SMiRT-12 / K. Kussmaul (Editor)

B06/2

A NONLINEAR FOUR NODE SHELL ELEMENT WITH EXPLICIT INTEGRATION AND ELEMENTARY ROTATIONS

B. Brank[1], D. Perić[2] and F.B. Damjanić[1]

[1]Departments of Civil Engineering, University of Ljubljana, Jamova 2, Ljubljana, Slovenia
[2]University College of Swansea, Swansea SA2 8PP, Wales, UK

Abstract – The nonlinear four node shell element, based on degenerated continuum concept is used in finite rotation shell analysis. Shell director rotation is described by elementary rotations dependant on two angles. Explicit integration through the thickness is performed, leading to the strain tensor, which includes coupling of curvature with displacements. Shell kinematics is consistently linearized. Typical benchmark tests are provided to illustrate the approach.

1. INTRODUCTION

The *four node* isoparametric shell finite element with bi-linear interpolation functions has been extensively studied. Our approach is related to the work of Stander et al. [1], Simo et al. [2-4] and Parish [5]. In these papers both a degenerated continuum approach and an implementation of Cosserat shell theory were considered in the regime of finite displacements and finite rotations. A close analogy of both formulations can be noticed, if the *explicit integration* through the shell thickness is performed in the former. Büchter and Ramm showed in [6] that explicit integration leads to the strain tensor, consistent with the first approximation of a geometrically non-linear shell theory for small strains including transverse shear deformation. The mid-surface curvature tensor is correctly represented and therefore does not produce the violation of the rigid body motion. Similar expressions for strains presented in [7] are obtained by the linear variation of Jacobian matrix across the shell thickness.

Large rotation formulation can be based either on elementary rotations, which are rotations around one axis (see for example [6]) or on rotational vector. The latter approach in shell analysis is described in detail in references [2-4] and [5]. We used elementary rotations, based on two angles presented by Ramm ([1], [6] and [8]). This kind of parametrization enables five nodal degrees of freedom. No need for the elimination of the drill rotation on the local level, which is frequently done in rotational vector formulation, therefore exist.

An important computational aspect of displacement type isoparametric elements is treatment of *membrane* and *shear locking* effects (see for example [3-4] for details). Numerical tests show ([3-4] ,[5]), that membrane locking of the 4-node element is not crucial due to lower order of interpolation and vanishes with finer meshes. The membrane and bending strain fields are therefore often (including the present work) approximated by standard bi-linear interpolation functions. However, better results are obtained with special treatment of membrane and bending strain fields, as shown in [3-4]. To avoid shear locking phenomenon, we used the assumed covariant transverse shear strain interpolation which

was originally proposed by Bathe and Dvorkin [9]. We analyse stresses and strains in a *local Cartesian coordinate system*, while in [1], [2-4] and [5], the curvilinear coordinate systems are used. This simplifies the constitutive equations.

From the computational point of view, an efficent algorithm with high rate of convergence is preffered. *Systematic linearization* of the shell kinematics leading to the Newton numerical procedure is therefore performed.

2. KINEMATICS OF THE SHELL

In the following we restrict attention to material description in terms of the *total Lagrange* formulation. θ^i (i=1,2,3) are curvilinear coordinates of the shell body and $\mathbf{E}_I$ (I=1,2,3) are unit base vectors of the *fixed Cartesian coordinate* system. Two basic assumptions; *linear variation of the displacements across the thickness* and *inextensional shell director* are introduced. The shell configuration can then be completely described by the position of the *mid-surface* and the *shell director*. The deformed and initial (reference) configuration of the shell are given by:

$$\mathbf{r}(\theta^i) = \mathbf{X}(\theta^\alpha) + \mathbf{u}(\theta^\alpha) + \theta^3 \mathbf{t}(\theta^\alpha), \qquad \mathbf{R}(\theta^i) = \mathbf{X}(\theta^\alpha) + \theta^3 \mathbf{T}(\theta^\alpha). \tag{1}$$

$-\frac{h}{2} \leq \theta^3 \leq \frac{h}{2}, \|\mathbf{t}\| = \|\mathbf{T}\| = 1$, Greek indices are either 1 or 2, h is the shell thickness, $\mathbf{X}$ denotes the mid-surface position at the reference configuration, $\mathbf{u}$ the displacement of the mid-surface, while $\mathbf{T}$ and $\mathbf{t}$ denote the shell director initial and deformed configuration, respectively. The covariant base vectors and *Green Lagrange strains* are given by:

$$\mathbf{g}_i = \frac{\partial \mathbf{r}}{\partial \theta^i}, \qquad \mathbf{G}_i = \frac{\partial \mathbf{R}}{\partial \theta^i}, \qquad \gamma_{ij} = \frac{1}{2}(\mathbf{g}_i \mathbf{g}_j - \mathbf{G}_i \mathbf{G}_j). \tag{2}$$

Using equation (1) in (2), one can obtain γ_{ij} as the quadratic function of θ^3. The standard assumptions which substantially simplify expression for γ_{ij} are often introduced at this stage. We reffer to [6] for details. Assuming small gradients of transverse shear strains, the quadratic terms of γ_{ij} can be neglected. Due to the assumption of the inextensional shell director, γ_{33} becomes zero and the transverse shear strains become independent on θ^3. The simplified expressions for the strain tensor can then be given:

$$\gamma_{\alpha\beta} = \varepsilon_{\alpha\beta} + \theta^3 \kappa_{\alpha\beta}, \qquad \gamma_{\alpha 3} = \gamma_\alpha, \qquad \gamma_{33} = 0. \tag{3}$$

The strains now take the form:

$$\varepsilon_{\alpha\beta} = \frac{1}{2}\Big(\mathbf{X}_{,\alpha}\mathbf{u}_{,\beta} + \mathbf{X}_{,\beta}\mathbf{u}_{,\alpha} + \mathbf{u}_{,\alpha}\mathbf{u}_{,\beta}\Big), \qquad \gamma_\alpha = \frac{1}{2}\Big(\mathbf{X}_{,\alpha}(\mathbf{t}-\mathbf{T}) + \mathbf{u}_{,\alpha}\mathbf{t}\Big),$$

$$\kappa_{\alpha\beta} = \frac{1}{2}\Big(\mathbf{X}_{,\alpha}(\mathbf{t}_{,\beta}-\mathbf{T}_{,\beta}) + \mathbf{X}_{,\beta}(\mathbf{t}_{,\alpha}-\mathbf{T}_{,\alpha}) + \mathbf{u}_{,\alpha}\mathbf{T}_{,\beta} + \mathbf{u}_{,\beta}\mathbf{T}_{,\alpha} + \mathbf{u}_{,\alpha}(\mathbf{t}_{,\beta}-\mathbf{T}_{,\beta}) + \mathbf{u}_{,\beta}(\mathbf{t}_{,\alpha}-\mathbf{T}_{,\alpha})\Big). \tag{4}$$

The *shell director* at the current ($\mathbf{t}$) and reference ($\mathbf{T}$) configuration is completely descibed by two angles ψ and ω (see Fig. 1a), which are denoted as Ψ and Ω at the reference configuration:

$$\mathbf{t} = \mathbf{R}_X(\psi)\,\mathbf{R}_Z(\omega - \frac{\pi}{2})\,\mathbf{E}_2, \qquad \mathbf{T} = \mathbf{R}_X(\Psi)\,\mathbf{R}_Z(\Omega - \frac{\pi}{2})\,\mathbf{E}_2. \tag{5}$$

$\mathbf{R}_X$ and $\mathbf{R}_Z$ are standard (3×3) rotational matrices which rotate Cartesian base around the axes defined by base vectors $\mathbf{E}_1$ and $\mathbf{E}_3$. Any position of the shell director is then determined by the rotation of $\mathbf{E}_2$ around $\mathbf{E}_1$, which is followed by the rotation around the new position of $\mathbf{E}_3$. This description helps to understand that angles at the deformed configuration can be evaluated by a simple summation of initial angles and the magnitude of the shell director rotations around axes $\mathbf{f}_\alpha$ and $\mathbf{f}_\beta$.

$$\psi = \Psi + \alpha, \quad \omega = \Omega + \beta, \qquad \mathbf{f}_\alpha = \mathbf{E}_1, \quad \mathbf{f}_\beta = \mathbf{E}_1 \times \mathbf{t}. \tag{6}$$

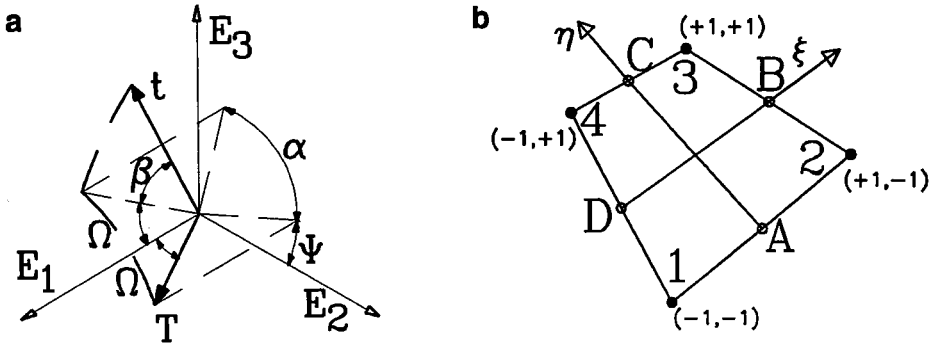

Fig. 1: a) Shell director at initial and deformed configuration. b) 4-node finite element.

3. THE WEAK FORM

The weak form can be expressed in the terms of Green-Lagrange strains and second Piola-Kirchoff stresses. Stresses are reffered to the shell mid-surface and therefore an assumption of constant thickness Jacobian is used. Stress integration across the thickness leads to the following expression:

$$G(\mathbf{r}, \delta\mathbf{r}) = \int_{S^o} (n^{\alpha\beta}\delta\varepsilon_{\alpha\beta} + m^{\alpha\beta}\delta\kappa_{\alpha\beta} + q^{\alpha}\delta\gamma_{\alpha})dS^o - G_{ext}(\delta\mathbf{r}). \tag{7}$$

$\mathbf{n}$, $\mathbf{m}$ and $\mathbf{q}$ are effective (symmetric) parts of the stress resultants. We reffer to [2] for details. In the present formulation the stresses are evaluated using equations (3) and constitutive relations which imply the *condensation of the material law* due to the assumption of *zero normal stresses*. Therefore the stress integration causes the integration of constitutive equations which for an *isotropic elastic material* leads to the well known factors Eh, $\frac{Eh^3}{12}$ and κGh. Equation (7) is non-linear due to the kinematic variables, therefore it is linearized in view of iterative solution methods. In this formulation the linearization is performed after the finite element discretization.

4. FINITE ELEMENT DISCRETIZATION

The geometry of the shell and kinematic variables are interpolated by bi-linear functions $N_i(\xi, \eta)$ (i=1,2,3,4). Mid-surface quantities are then approximated:

$$\mathbf{X} = \sum_{i=1}^{4} N_i \mathbf{X}_i, \qquad \mathbf{u} = \sum_{i=1}^{4} N_i \mathbf{u}_i, \qquad \mathbf{T} = \sum_{i=1}^{4} N_i \mathbf{T}_i, \qquad \mathbf{t} = \sum_{i=1}^{4} N_i \mathbf{t}_i. \tag{8}$$

At each node the reference director $\mathbf{T}_i$ is obtained by *averaging* the nodal normals of adjoining elements. Element nodal normal is given by the vector product of the corresponding

element edge vectors. Another alternatives of specifying nodal directors are much more impractical (by two points on top and bottom surface for example). The derivatives of mid-surface quantities are interpolated by the the shape functions derivatives. Note, that the components of the shell director are interpolated rather than rotational variables α and β. In [6] better results are reported, if the rotational variables are interpolated explicitly. The another interpolation of shell director field, which enforces it to unit lenght throughout the element, is described in [3], but it is not used in non-linear analysis [4]. In addition, the transverse shear strain field is given by constant-linear interpolation as originally proposed in [9]. Strains from eq. (4) are evaluated only at the points A, B, C and D. (See Fig. 1b.)

$$\gamma_1 = \frac{1}{2}(1+\eta)\gamma_1^A + \frac{1}{2}(1-\eta)\gamma_1^C, \qquad \gamma_2 = \frac{1}{2}(1+\xi)\gamma_1^D + \frac{1}{2}(1-\xi)\gamma_1^B. \tag{9}$$

Using upper interpolation in equations (4) the *discrete formulation* of the weak form (7) can be evaluated. Assuming the conservative loading, the tangent stiffness operator can be obtained by the directional derivative of the internal virtual work. On the element level the tangent operator may be conventionally split into material and geometric part:

$$DG^e(\mathbf{r}, \delta\mathbf{r}) \cdot \Delta\mathbf{r} = D_M G^e(\mathbf{r}, \delta\mathbf{r}) \cdot \Delta\mathbf{r} + D_G G^e(\mathbf{r}, \delta\mathbf{r}) \cdot \Delta\mathbf{r}. \tag{10}$$

The directional derivative of the shell director is given by:

$$D\mathbf{t}(\psi, \omega) \cdot \Delta\mathbf{t} = \mathbf{t}_\alpha \alpha + \mathbf{t}_\beta \beta, \tag{11}$$

where $\mathbf{t}_\alpha$ and $\mathbf{t}_\beta$ can be evaluated from equations (5) and (6) by considering the properties of the directional derivative.

5. NUMERICAL EXAMPLES

Two standard benchmark tests are presented. In all examples a tangent stiffness matrix is calculated for each iteration.

EXAMPLE 1: Pinched hemispherical shell with 18^o *hole.* The loading and boundary conditions are shown in Fig. 2a. The material properties are $E = 6.8257 \times 10^7$, $\nu = 0.3$, radius $R = 10$ and thickness is $t = 0.04$. The analysis was performed for one quarter of the shell. Two different meshes A (8×8) and B (16×16) were considered. The check of the residual forces was performed with convergence tolerance 1.0×10^{-7}. Pinched forces were applied in 40 equal load steps up to $F_{tot} = 400$. Upper two curves at the Fig. 2c correspond to the displacements in X_2 direction, while lower two curves represent the displacements in X_3 direction. Displacements at $F = F_{tot}$ are 3.925 and 7.684 for mesh B. The quadratic rate of asymptotic convergence with 4 to 7 iterations at each load step was reached, leading to the total number of 193 iterations. Coarser mesh A behaves considerably stiffer.

EXAMPLE 2: Pinching of a clamped cylinder. The problem details are shown at Fig. 3a. The material properties are $E = 2.0685 \times 10^7$ and $\nu = 0.3$. One quarter of the shell was analysed, considering the symmetry restrictions. The pinched loads were applied at the free end and 20 equal load steps were used to arrive at the configuration at $F_{tot} = 1600$. Convergence tolerance for residual forces was set to 1.0×10^{-7}. A mesh of (16×16) was considered and 4 to 12 iterations were required at each load step, leading to the total number of 150 iterations. Displacement at point A is equal to 1.608 at $F = F_{tot}$. Note, that the largest phisically possible displacement is equal to radius.

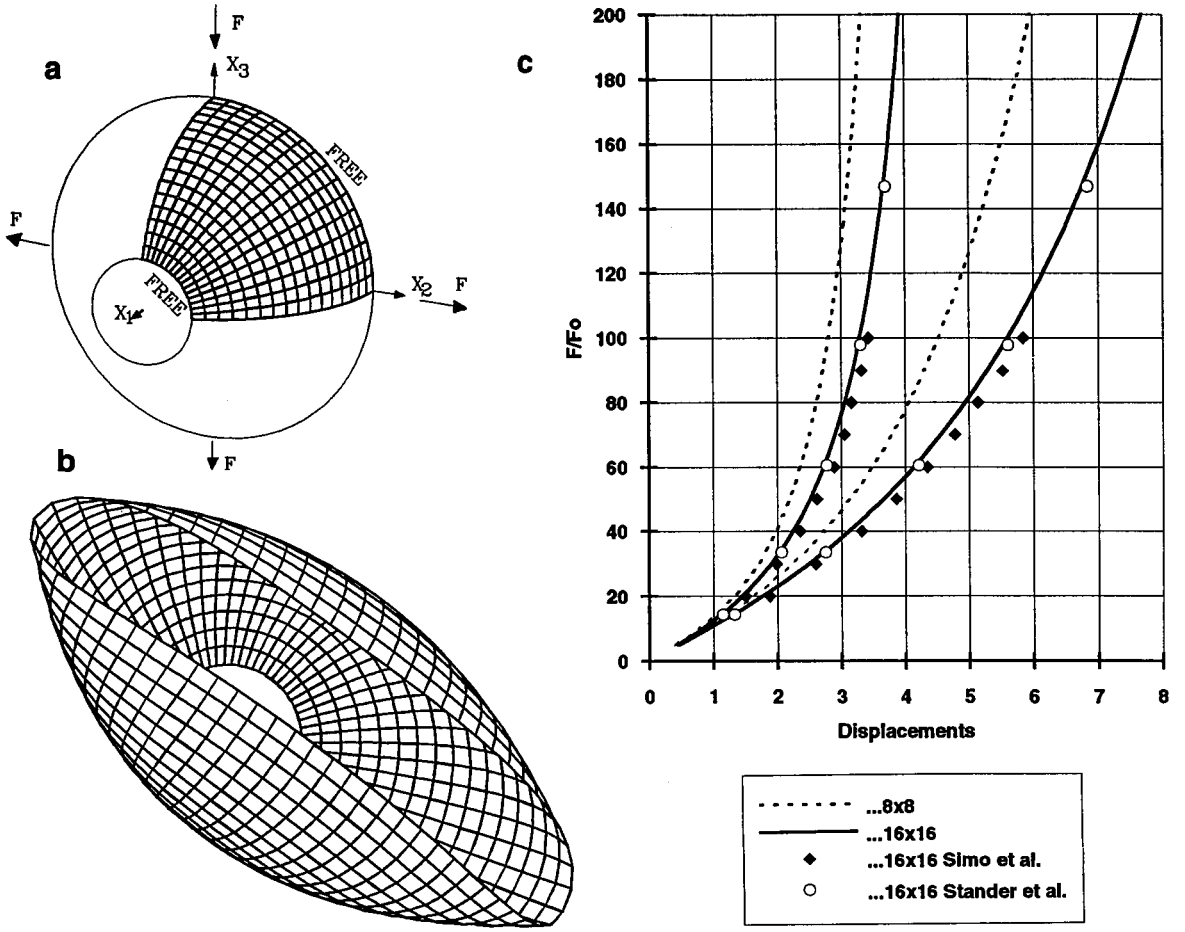

Fig. 2: a) Initial mesh B and the problem data. b) Deformed mesh at $F = F_{tot}$. c) Load versus displacements curves for points under the forces.

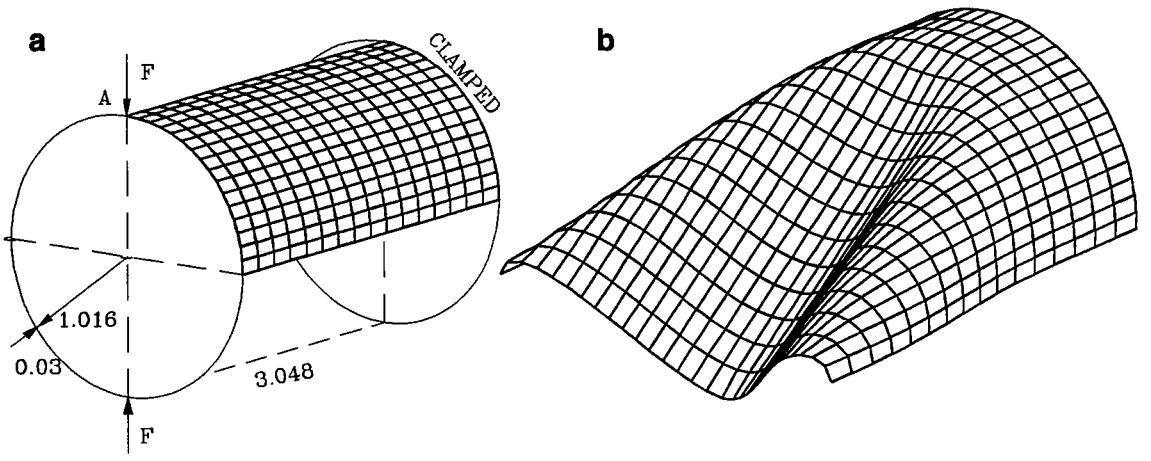

Fig. 3: a) Initial mesh and the problem data. b) One half of the cylinder at the $F = F_{tot}$.

6. CONCLUSION

The four node resultant stress shell finite element is used in finite rotation shell analysis. Large rotation formulation is based on two angles presented by Ramm ([1],[6],[8]).

Systematic linearization of the adopted model has been performed, leading to an effective numerical algorithm, which exibits a quadratic rate of asymptotic convergence. Using the formulation presented some typical benchmark tests have been succesfully completed. However, better results are expected with more precise interpolation of rotational variables. We can conclude that the 4-node shell element with explicit integration and elementary rotations in general exibits similar behaviour to the displacement based 4-node elements described in [2-4,5].

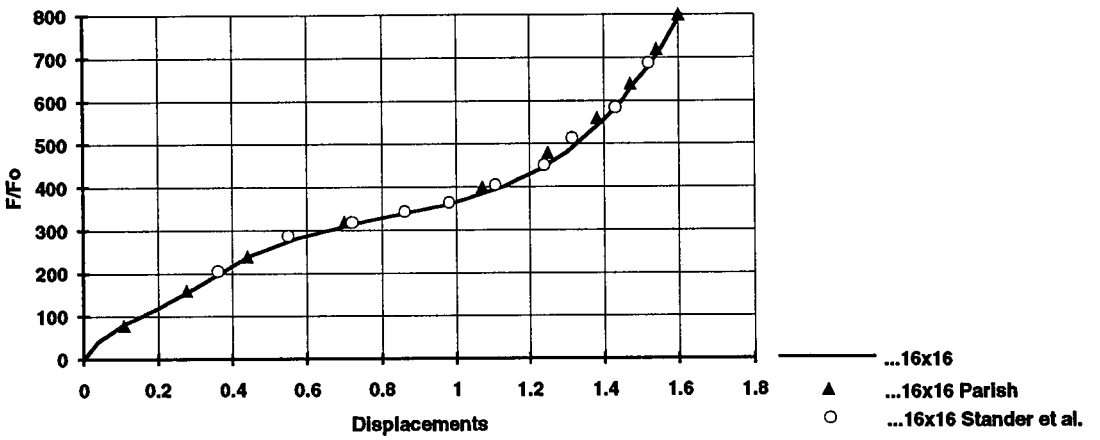

Fig 4: Clamped cylinder: load versus displacement curve for point A.

Acknowledgments – The first author wishes to thank The Ministry of Science and Technology of Slovenia for the financial support. The TEMPUS grant for three months staying at the University College of Swansea is also gratefully acknowledged.

7. REFERENCES

[1] Stander, N., Matzenmiller, A., Ramm, E. 1989. An assesment of assumed strain methods in finite rotation shell analysis. Eng. Computations 6: 57-66.

[2] Simo, J.C., Fox, D.D. 1989. On a stress resultant geometrically exact shell model. Part I: Formulation and optimal parametrization. Comp. Methods Appl. Mech. Eng. 72: 267-304.

[3] Simo, J.C., Fox, D.D., Rifai, M.S. 1989. On a stress resultant geometrically exact shell model. Part II: The linear theory. Comp. Methods Appl. Mech. Eng. 73: 53-62.

[4] Simo, J.C., Fox, D.D., Rifai, M.S. 1990. On a stress resultant geometrically exact shell model. Part III: Computational aspects of the nonlinear theory. Comp. Methods Appl. Mech. Eng. 79: 21-70.

[5] Parish, H. 1991. An investigation of a finite rotation four node assumed strain shell element. Int. J. for Numer. Methods in Eng. 31: 127-150.

[6] Büchter, N., Ramm, E. 1992. Shell theory versus degeneration - a comparison in large rotation finite element analysis. Int. J. for Numer. Methods in Eng. 34: 39-59.

[7] Belytschko, T., Wong, B.L., Stolarski, H. 1989. Assumed strain stabilization procedure for the 9-node Lagrange shell element. Int. J. for Numer. Methods in Eng. 28: 385-414.

[8] Ramm, E., Matzenmiller, A. 1986. Large deformation shell analysis based on the degeneration concept in Finite Element Methods for Plate and Shell Structures (ed. T.J.R. Hughes, E. Hinton), Swansea: Pineridge press.

[9] Dvorkin, E.N., Bathe, K.-J., 1984. A continuum mechanics based four-node shell element for general non-linear analysis. Eng. Comput. 1: 77-88.